ELSEVIER

15 December 1998

OPTICS COMMUNICATIONS

Optics Communications 158 (1998) 305–312

Full length article

Narrow-line-width diode laser with a high-*Q* microsphere resonator

V.V. Vassiliev [a,*], V.L. Velichansky [a], V.S. Ilchenko [b], M.L. Gorodetsky [b], L. Hollberg [c], A.V. Yarovitsky [a]

[a] *P.N. Lebedev Physics Institute, Moscow 117924, Russian Federation*
[b] *Physics Department, M.V. Lomonosov State University, Moscow 119899, Russian Federation*
[c] *NIST, Boulder, CO, USA*

Received 4 June 1998; revised 11 September 1998; accepted 15 October 1998

Abstract

A new modification of external optical feedback (OFB) was used to narrow the line of a diode laser (DL). A 'whispering gallery' (WG) mode of a high-*Q* microsphere was excited by means of frustrated total internal reflection while the feedback for optical locking of the laser was provided by the intracavity Rayleigh backscattering. The ~ 600 MHz beatnote of the two laser diodes optically locked to a pair of orthogonally polarized modes of the same microresonator had the indicated spectral width of 20 kHz, and the stability of 2×10^{-6} over averaging time of 10 s. The feasibility of miniature sub-kHz-line width laser is discussed.

PACS: 42.55.Px; 42.60.Jf
Keywords: Optical feedback; Line width reduction; Frequency stability; High-*Q* microresonator; Whispering-gallery modes

1. Introduction

With modern efficient and reliable techniques to narrow the line width of diode lasers (DL) at increasing output powers, DL can compete with and replace conventional gas and dye lasers in metrology and high-resolution spectroscopy [1]. Unlike electronic methods for reducing the line width, optical feedback (OFB) can easily provide broadband suppression of DL frequency noise. Two main modifications of the OFB technique include: (1) extended cavity oscillation [2,3] with anti-reflection (AR) coating of one of the DL facets and (2) weak coupling to an external high-finesse cavity [4,5]. In the first case, the laser cannot oscillate without external grating (mirror), and the finesse of the compound cavity is limited by efficiency of the coupling to the active region (0.01–0.5). In the second modification, the free-running DL is well above threshold, and optimal frequency stabilization is achieved with weak OFB ($< 10^{-4}$).

Of the two modifications, external high-*Q* cavity OFB technique provides higher output power and better short-term stability, and also does not require AR coating of the DL. Most frequently used cavities are confocal Fabry–Perot [4,5] and fiber ring resonators [6,7]. Despite the advantages, external high-*Q* cavity systems are complex and used only in laboratories, while strong OFB tunable systems are now available commercially [8,9].

Normally, achievement of high *Q*-factor of external cavity leads to substantial increase of DL system dimensions. Few attempts have been reported to create a compact external high *Q*-cavity-stabilized DL. For example in Ref. [9], a 10-mm glass hemisphere was used as external Fox–Smith cavity [10], and in Ref. [11] an external Bragg reflector was integrally built and coupled to a DL within

* Corresponding author. Tsentralnaya str. 26-17, 142092, Troitsk, Moscow Region, Russian Federation. E-mail: vvv@x4u.lebedev.ru

0030-4018/98/$ - see front matter
PII: S0030-4018(98)00578-1

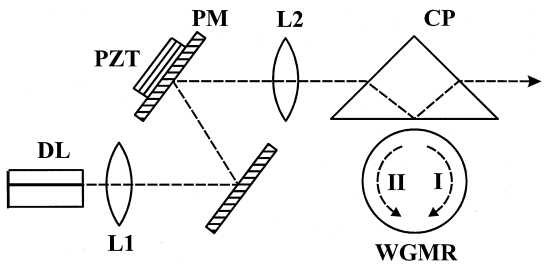

Fig. 1. The basic scheme of a DL coupled to a WG microresonator. DL – diode laser; L1 – collimating lens; PM, PZT – phase mirror mounted on a piezoelement; L2 – focusing lens; CP – coupling prism; WGMR – whispering gallery microresonator.

the same chip. However, reduction of dimensions of conventional optical cavities compromises their Q and diminishes the resulting laser coherence.

In this paper, we report on the application of the weak OFB technique to an optical resonator that combines submillimetre dimensions and $Q \geq 10^9$ [12,13] – fused-silica microsphere resonator with whispering-gallery modes (WGMR). In our experiment, WGMR was coupled to a DL as follows (Fig. 1). The DL radiation collimated by the first lens L1 is then focused by coupling lens L2 onto the inner surface of the coupling prism. The WGMR is placed at a distance (of the order $\lambda/2\pi$) from the focal spot, and frustrated total internal reflection (TIR) enables excitation of circular WG mode in the sphere (travelling-wave I). Intracavity backscattering effect in high-Q cavity leads to the build-up of backward circular wave II which is then outcoupled by the prism coupler and sent back to the laser.

The DL is operated well above its threshold in single-mode regime; the phase mirror adjusts the phase of the feedback at optimum similarly to that in Refs. [4,5]; feedback level is limited to the optimal value less than 10^{-4} by adjusting microsphere–prism gap and/or attenuator; with larger feedback oscillation becomes unstable [14].

2. A probe-reference laser

A probe-reference laser was used to observe spectra of WG modes, to measure Q-factor of the WGMR, and to estimate the line width of the laser under study. Two loops of OFB were employed [15,16]. A strong-OFB loop was formed by a diffraction grating (1302 grooves/mm, 60% efficiency) mounted in Littrow configuration. The coupling objective had a numerical aperture of $N_A = 0.65$. The length of the cavity was 3 cm. Since both optical facets of the laser diode were accessible, the two output beams delivered powers of 3 and 2 mW (at 852 nm) after the output objective and in the 0th order of the grating, respectively. The grating was mounted on two PZTs, which provided matched rotation and translation of the grating. Together with synchronous ramp modulation of pumping current it gave the continuous tuning range of 280 GHz. Fig. 2a displays the extended portion of the reemitted WG mode spectra taken with the ECDL. Transmission of the reference Fabry–Perot etalon being recorded simultaneously (Fig. 2b) proves truly continuous tuning of the lasing frequency and reveals monotonic power change resulting from the current ramp. The cut of 170 GHz shows approximately the free spectrum range of the WGMR evaluated from the dimensions of the sphere.

The line width of the described ECDL was about 800 kHz. It was further reduced with a second OFB loop which provided weak coupling to a confocal cavity with free spectrum range (FSR) and finesse being 300 MHz and 75, respectively. The active stabilization of the distance between the ECDL and the confocal cavity was accomplished by modulation of this distance and by using a standard servoloop [4]. The laser with two loops of OFB combines tunability (controlled by grating) with better stability and reduced line width (due to high-finesse cavity). By using this laser as a local oscillator in heterodyne measurement of the line width of DL coupled to the microresonator we have found the beatnote width of less than 100 kHz [17].

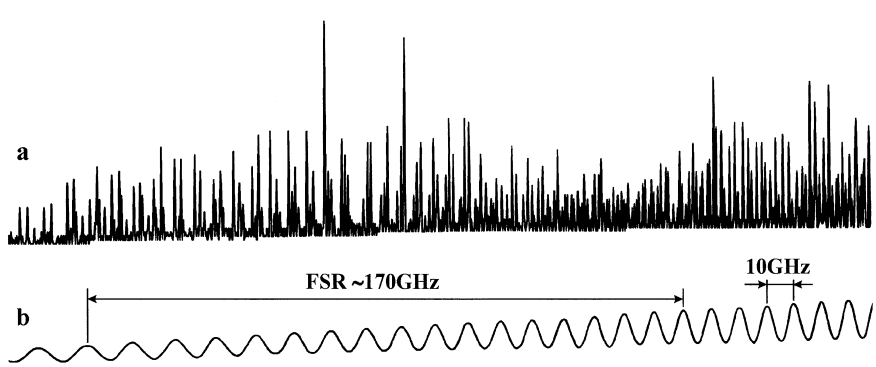

Fig. 2. The WG mode spectrum (a) and transmission of the reference etalon (b). The horizontal scale is not linear due to nonlinear response of the piezoelements. The digitizing steps of the digital oscilloscope are the origin of the small jumps in the base line of (a).

3. Microsphere resonator with 'whispering gallery' modes

The microcavity was made of fused silica in the flame of an oxygen–hydrogen torch. It was then put into a hermetic chamber to protect it from dust and condensates (which lead to the deterioration of the Q-factor) and to prevent temperature variations produced by air flows. The FSR of the microresonator was $\Delta_0 = c/(\pi D n_s) = 178$ GHz ($D = 370$ μm is the diameter of a microsphere, and $n_s = 1.45$ is the refractive index of fused silica at 852 nm). The BK-7 glass coupling prism was mounted in the same chamber. The gap between coupling prism and the sphere was controlled by a microtranslation stage.

The eigenmodes of a dielectric sphere are characterized by polarization and three indices [18]: l, m, and q where l is close to the number of wavelengths that fit into the optical length of the 'equator', m equals the number of field maxima in the equator plane, and $q \geq 1$ is the number of field maxima in the direction along the radius of the sphere. The WG modes are specified by the condition $l \gg q$. Their Q-factors become very high for low-loss material (fused silica) and large radius of the sphere ($R \geq 30\lambda$) where radiative losses become small. In the ideal sphere, modes are degenerate with respect to the index m. The fused silica microresonators obtained by current fusion technology are not ideal spheres and their shape is closer to that of an ellipsoid. The mode spectrum of such a configuration was analyzed in Ref. [19]. With the eccentricity of the microsphere being $\varepsilon = \sqrt{a^2 - b^2}/a$ (a, b are axes of the ellipsoid) and at $l \gg l - |m|$ the eigenfrequencies are given by (see also Ref. [20]):

$$\gamma_{qlm}^{E,H} = \Delta_0 \left[l + 1/2 - A_q \sqrt[3]{(l+1/2)/2} - \Delta_{E,H} \pm \varepsilon^2 (l - |m|)/2 \right], \quad (1)$$

where the positive sign stands for the oblate spheroid and negative sign corresponds to the stretched one.

The A_q numbers are qth zeros of Airy function and for the first $q = 1$–5: $A_q = 2.338$; 4.088; 5.521; 6.787; 7.944. The greatest change of frequency is produced by variation of q. Note that for large spheres $l \gg 1$ A_q is multiplied by a factor, which in our case is about 10, so that $\nu_{2lm}^{E,H} - \nu_{1lm}^{E,H} \approx 17.5\Delta_0$. The distance between adjacent q-modes decreases with q, but the first four mode separations are all greater than $10\Delta_0$ for $l \sim 2000$. Simultaneous variations of l and m ($l = m$) produce a quasi-equidistant mode family separated by $\approx \Delta_0$. On increasing l by 10 in the vicinity of $l = 1960$ the mode separation becomes only about 4% greater due to the term $A_q \sqrt[3]{(l+1/2)/2}$. Note that the deviation from equidistant mode separation is proportional to $|A_q|$ and increases with q.

The last term in Eq. (1) shows that m-degeneracy is removed for a nonideal sphere in which case the $l - |m| + 1$ number determines the number of field maxima in the meridional direction [19]. The mode family specified by $q, l = \text{const}$ and different m is equidistant provided that $l - |m| \ll l$. The minimum mode separation for this family is $\Delta_0 \varepsilon^2/2$ and depends on the shape of the microcavity with typical values of $\varepsilon^2/2$ being 5×10^{-2}–5×10^{-3}. This family has the highest density of modes. The whispering waves of the two orthogonal polarizations have different confinements and effective refractive indices. As a result the spectra for both polarizations are shifted to low frequencies (in Δ_0 units) by $\Delta_E = 1/\beta$ and $\Delta_H = (1 - \beta^2)/\beta$ for TE and TM modes, respectively, where $\beta = \sqrt{n^2 - 1}/n$ (we assume here that the refractive index of the air is 1). The mode spectrum of the microcavity is presented in Fig. 2a as peaks of light reemission from the sphere into the coupling prism. The spectrum is rather involved which corresponds to the complicated hierarchy of mode families. The free spectrum range is not actually 'free'. We note that even in the case of an ideal sphere the WGM spectrum is far from being simple: the free spectrum range defined by $\nu_{1,1959} - \nu_{1,1958}$ contains for instance the following [q, l] modes: [2, 1941], [3, 1927], [4, 1914], [5, 1903]. The high density of observed spectra implies that: (1) Q-factors of the modes do not decrease fast with q (the $q^{-1/2}$ scaling was used in Ref. [20]) and $l - |m|$

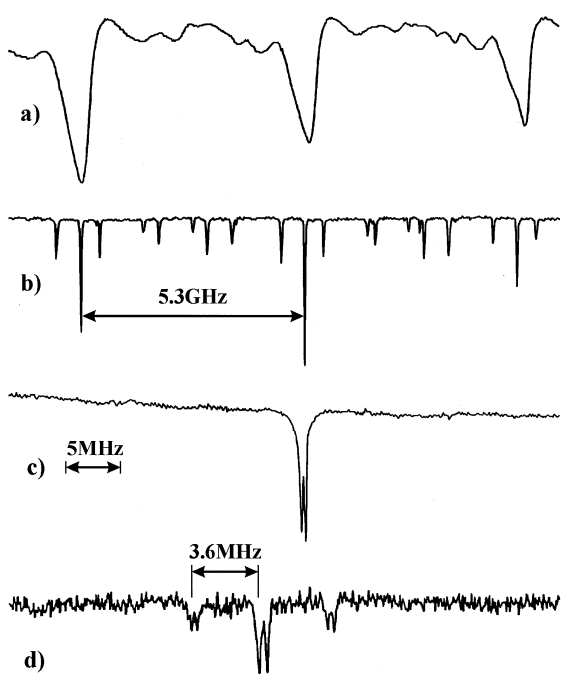

Fig. 3. Part of the WGM spectrum. Displays (a) and (b) are taken at the same scale but for different distances between prism and sphere (d for (a) is smaller); (c) gives central mode of (b) taken at much greater resolution (the scale is stretched by about 500 times); (d) the same mode as in (c) at smaller coupling. The RF modulation at 3.6 MHz gives the scale.

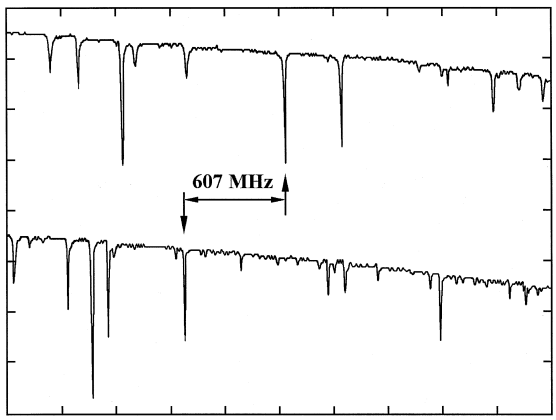

Fig. 4. Two sets of whispering-gallery modes for the orthogonal polarizations. Arrows show the modes used for the optical locking of the two laser diodes.

numbers; (2) there are many high-Q reference lines available for frequency stabilization and by slight variation of temperature ($\approx 3°C$) any wavelength can be covered by some of them. Series of equidistant modes separated by $\Delta_0 \varepsilon^2 = 5.3$ GHz can be distinguished in the spectrum shown in Fig. 3b from which we found $\varepsilon = 0.25$. It is predictable that very small ε values can result in overlapping of the modes and consequently their broadening.

The fragments of spectra for two linear and orthogonal polarizations are presented in Fig. 4 in the same absolute frequency scale. A great choice of frequency differences between the orthogonally polarized modes is available. In the present work we were interested in high density spectra and did not try to rarefy them by a proper tailoring of the beam shape and excitation angles. It is known, however, that both high l–m and q modes can be suppressed in this way [19] [1].

The spectra presented so far were taken with a reference laser in a simple, single OFB-loop configuration which provides large tuning but not the ultimate resolution. Now we turn to the measurements of Q where both OFB-loops of the laser were activated.

4. Measurements of the quality factor

The internal losses of silica microresonator are very small compared to maximum losses via prism coupler at $d = 0$ (the coupler-microresonator gap value). Hence the Q-factor of the loaded microresonator can be several orders of magnitude smaller than that of the unloaded cavity. Fig. 3a–d shows evolution of spectra as the distance between the prism and the sphere increases. First a mode narrows, then it splits into two lines and eventually stops to depend on d practically which means that losses due to reemission from the sphere into the prism become negligible (undercoupled regime).

The line of the undercoupled cavity (Fig. 3d) reveals splitting that comes from the coupling between forward and backward waves arising due to the Rayleigh backscattering [21,22]. Small satellites on each side of the principal resonance are the frequency marks produced by means of RF phase modulation of the input beam. The measured width of a separate resonance was 370 kHz corresponding to the microresonator Q-factor of 0.96×10^9. This measurement was made when the sphere was 6 months old. It was kept in a hermetic (but not vacuum) chamber.

It is interesting to measure not only the maximum Q, but also the value of Q which provides the greatest locking range of a DL to a whispering-gallery mode. The wave that returns to the laser from the sphere is formed due to Rayleigh backscattering and becomes appreciable only if the propagation length in the sphere is large enough. Thus, it is clear that optimum feedback condition should correspond to some intermediate value of Q (and the gap): if Q is too large ($d \geq \lambda$) the coupling efficiency is very small. That is, the condition for Rayleigh backscattering is optimum, but there is no energy exchange between the sphere and the prism. On the other hand if d goes to zero, coupling efficiency increases but the efficient length of wave propagation inside the sphere is not sufficient for energy transfer to counter-propagating wave. The low Q diminishes also the locking range of the DL and the line width reduction ratio.

The optical scheme for the Q-factor measurement under the optimum loading condition is illustrated in Fig. 5. The diode laser (Spectra Diode Lab, type SDL-5401-G1,

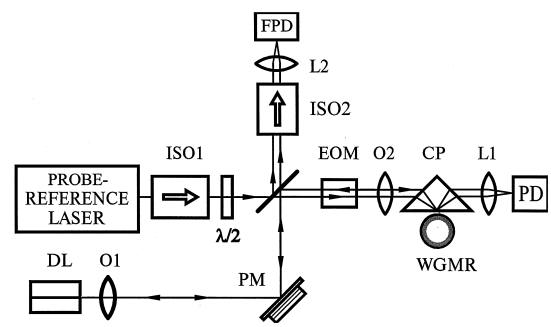

Fig. 5. The experimental setup for the Q-factor measurements under the optimum locking conditions. DL – diode laser; O1 – collimating objective; PM – phase mirror; ISO1, ISO2 – optical isolators; $\lambda/2$ – half-wave plate; L1, L2 – lenses; EOM – electrooptical modulator; O2 – focusing objective; CP – coupling prism; WGMR – whispering-gallery microsphere resonator; PD – photodiode; FPD – fast photodiode.

[1] We have recently displayed spectra of a greater sphere ($\Delta_0 =$ 110 GHz) in a continuous range of 360 GHz with a better angular control of exciting beam. In that case periodical variations of spectra corresponding to FSR are distinguished and at least partial identification of modes is possible. These results will be published elsewhere.

line width 15 MHz, output power 20 mW after the objective with $N_A = 0.5$, $\lambda = 852$ nm) was optically locked to one of the WG modes. The locking range was then measured for different d and the OFB phase was optimized in each measurement. The beams of the reference laser and the laser under study were combined on a beam splitter in such a way that they had the same polarizations, frequency, direction and spatial position. Therefore, the probe-reference laser was tuned to the same WGMR resonance. The output polarization of the probe laser was adjusted by means of a half-wave plate; its frequency was examined by the beatnote of the two lasers; and an electro-optical modulator (EOM) produced frequency marks. After optimum alignment the laser under study was blocked and the mode width was measured directly by tuning the probe laser.

The width of the WGMR resonance under the optimum loading conditions was within the range of values from 1 to 6 MHz for a number of modes which were efficiently excited and revealed high unloaded Q. These values coincide in order of magnitude with the resonance widths of the confocal cavities that had been used in Refs. [4,5] for the spectral narrowing of the laser diodes. However, the linear dimension of the microresonator is 100–1000 times smaller than that of the traditional cavities.

5. Simultaneous optical locking of two DLs to WG modes with orthogonal polarizations

Fig. 6 demonstrates the setup used to lock two independent DLs to the orthogonally polarized modes of the same

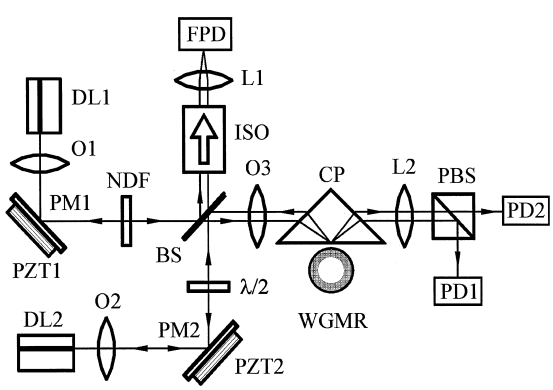

Fig. 6. The setup for locking of two lasers to orthogonally polarized modes of the microsphere. DL1,2 – diode lasers; O1,2 – collimating objectives; PM1,2 and PZT1,2 – phase mirrors mounted on piezoelements; NDF – neutral density filter (attenuator); $\lambda/2$ – half-wave plate; ISO – optical isolator; BS – beamsplitter; L1,2 – lenses; FPD – fast photodiode; O3 – focusing objective; CP – coupling prism; WGMR – whispering-gallery microsphere resonator; PBS – polarizing beamsplitter; PD1,2 – photodiodes.

microsphere. These modes are marked by arrows in Fig. 4. Orthogonal polarizations were chosen to suppress the crosstalk between the lasers and to enable their independent control. The laser beams were combined by means of the nonpolarizing beam splitter (BS) with reflection coefficient of 30%. As in the case of usual confocal cavities the lasers became unstable at large feedback level [4,5,14]. Direct measurements showed that it happened at the level of about 10^{-4} (as measured in the collimated beam returning to the laser). The efficiency of coupling into the active region is not taken into account. Thus, the real feedback could be 3 to 10 times smaller. To decrease it for DL2 the prism–sphere distance was increased to the optimum value. For a given beam splitter and relative orientation of the laser polarizations further suppression of feedback level was needed for a DL1 which was accomplished by attenuator (NDF). The beams of the lasers emerging from the microcavity were separated by a polarizing beam splitter (PBS, extinction ratio $> 10^3$) and were used for the stabilization of the corresponding feedback phases.

The beatnote of the two lasers spectrally narrowed by using the feedback from the WGMR is displayed in linear and logarithmic scales (Fig. 7a and b, respectively) and shows that the line width of an individual laser does not exceed 20 kHz. The analysis of the beatnote spectrum reveals that in the region of high Fourier frequencies it is well described by a Lorentzian (see the fit in Fig. 7b), while an additional spectral broadening is clearly observed at frequencies below 50 kHz. Thus, the laser spectrum might be represented as a narrow line of Lorentzian shape experiencing low-frequency perturbations. The central part of the line may contain contributions from: (1) technical noises; (2) FM modulation which accompanies stabilization of the laser–microsphere distance; (3) the resolution of the spectrum analyzer (resolution of 10 kHz was imposed by the drift of the beatnote frequency). According to the specifications of the spectrum analyzer its roll-off is much steeper than that of the Lorentz function. It is unlikely that the first two sources contribute to the far wings of the beatnote spectrum, and we consider them to be determined by the convolution of the laser lines. Taking into account the results of Ref. [5] we made a fit of the wings to $(1+X)^{-N}$, with $X = (2\Delta\nu/\Gamma)^2$ where $\Delta\nu$ is the detuning and $\Gamma\sqrt{(2^{1/N}-1)}$ is the line width (FWHM). The shape of the far wings ($X \gg 1$) is not sensitive to Γ but depends on N. We found that the fit was equally good for $N = 1, \ldots, 3/2$ (it was closer to $N = 3/2$ in Ref. [5]) and became very fast inadequate out of this range. Taking the peak value from the measurement and assuming a Lorentz function ($N = 1$), we get $\Gamma \approx 800$ Hz. Since all the noise sources described above, which broaden the central part of the line, can only decrease the peak value and the dropout, from the peak to the Lorentz wing we arrive at the estimates ranging between $\Gamma \leq 0.8$ kHz for $N = 1$ and $\Gamma \leq 4$ kHz for $N = 3/2$. These values are in good agreement with the 2 kHz prediction one can infer

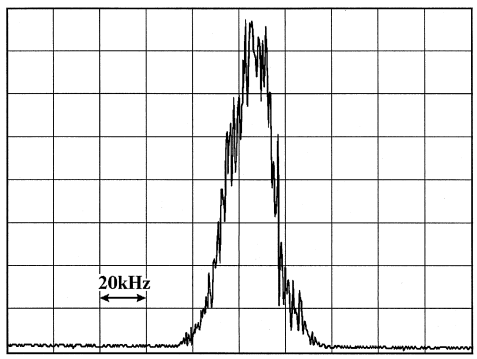

a)

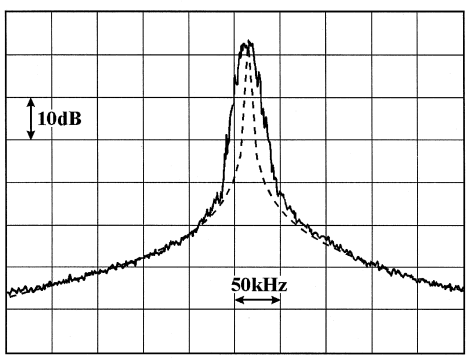

b)

Fig. 7. The beatnote spectrum of two DLs optically locked to the orthogonal modes of the WGMR. (a) Linear scale, frequency span 200 kHz, resolution 10 kHz, sweep time 5 s, video bandwidth 30 Hz. (b) Logarithmic scale, frequency span 500 kHz, resolution 10 kHz, sweep time 10 s, video bandwidth 30 Hz. The dashed curve is the Lorentzian best fit with FWHM of 790 Hz.

from the 20 MHz line width of the free-running laser and the observed stabilization coefficient (the ratio of current-to-frequency tunability with and without OFB from WGMR) [17].

6. The beatnote stability

Fig. 8b shows Allan variance of the beatnote frequency (607 MHz). For the sampling time of up to 1 min the stability remains better than 4×10^{-6} (it becomes 10^{-12} if the optical frequency is used for normalization, however correlated perturbations of the two frequencies are not taken into account), and then it starts to rise due to the monotonic drift of the beat frequency. A typical result for a direct measurement of the drift is shown in Fig. 8a. It gives the value of 40 kHz per 1000 s. In what follows we consider three possible contributions to the drift: (1) variation of the microsphere temperature; (2) change of the prism–microsphere distance; (3) different shifts of laser frequencies with respect to the reference lines of the microcavity.

(1) If the frequency difference of two orthogonal modes were defined only by the relative change of optical lengths $\delta\nu/\nu=-\delta(n_sL)/(n_sL)$ the variation of the beat frequency would be $(1/\delta\nu)(\mathrm{d}(\delta\nu)/\mathrm{d}T)=-(1/n)(\mathrm{d}n/\mathrm{d}T)-(1/L)(\mathrm{d}L/\mathrm{d}T)$. The first term is dominant and gives $\delta\Delta\nu/\Delta\nu=-7\times10^{-6}\delta T$. The temperature of the chamber was not actively stabilized but the drift of the room temperature was not greater than 0.5 K per 15 min. Thus, variation of frequency during this time should not exceed 2 kHz while the measured drift was 20 times greater. The given estimate refers, however, to the modes of the same polarization.

The situation is different for two orthogonally polarized modes. As (1) shows the spectra for two polarizations are identical but shifted by $\nu^H_{qlm}-\nu^E_{qlm}=\Delta_0\,\beta=125$ GHz. The beatnote was observed at much smaller frequency of $\delta\nu=0.6$ GHz. This is only possible if the WGMs that we used for locking had different sets of mode indices (qlm and $q'l'm'$). Hence, we have for the beat frequency:

$$|\delta\nu|=\left|\nu^H_{q'l'm'}-\nu^E_{qlm}\right|=\left|\left(\nu^H_{qlm}-\nu^E_{qlm}\right)-\left(\nu^H_{qlm}-\nu^H_{q'l'm'}\right)\right|$$
$$=\Delta_0|\,\beta-G|.$$

Here $\nu^H_{qlm}-\nu^E_{qlm}=\Delta_E-\Delta_H=\beta\Delta_0$, and G is determined by two sets of integer numbers (qlm and $q'l'm'$)

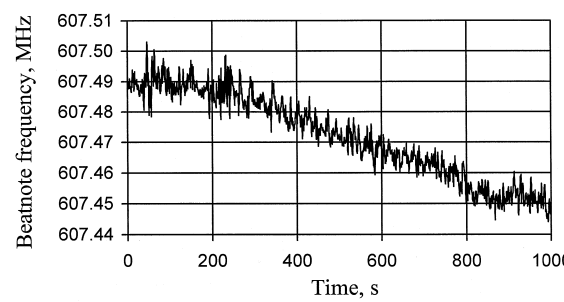

a)

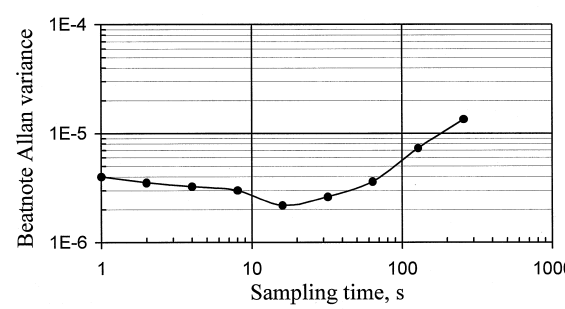

b)

Fig. 8. The time dependence of the beatnote frequency (a); Allan variance of the beatnote frequency (b).

and by ε, and does not depend on temperature. While $\beta - G = \delta\nu/\Delta_0$ is a small number ($\approx 3\times 10^{-3}$) both β and G are much greater ($\beta = 0.724$). Thus, $\delta\nu$ is a small difference of two large values with different temperature dependences, and its change with temperature becomes much greater:

$$\frac{\mathrm{d}|\delta\nu|}{\mathrm{d}T} = \pm\frac{\Delta_0}{n}\frac{\mathrm{d}n}{\mathrm{d}T}\left(\frac{1}{n\sqrt{n^2-1}} - (\beta - G)\right) \qquad (2)$$

with '+' and '−' corresponding to $\beta > G$ ($\nu^H > \nu^E$) and $\beta < G$ ($\nu^H < \nu^E$) cases, respectively. The second term refers to the discussed above case of small difference in optical length of the modes. The first term is much greater since $(1/n\sqrt{n^2-1})(1/|\beta - G|) \approx 200$. Thus for small beatnote frequencies the relative change of $\nu^E - \nu^H$ with temperature can be much greater than $(1/n)(\mathrm{d}n/\mathrm{d}T)$ which can be used in temperature sensors. The absolute value of frequency difference increases with temperature ('+' in Eq. (2)) for $\beta > G$ and decreases in the opposite case. Indeed, by slight changing the alignment and relocking the lasers it was easy to get a different beat frequency (say 400 MHz) with the opposite sign of the drift.

On the other hand the two terms in Eq. (2) have opposite signs at $\beta > G$, and on choosing greater separation between the modes, so that $G = \beta - n^{-1}(n^2-1)^{-1/2} \approx 0.067$ they can be made to compensate each other. In this way the relative change of $\mathrm{d}(\delta\nu)/\delta\nu$ with temperature can be made smaller than $10^{-8}/°\mathrm{C}$. For available diameters of the spheres of $D \sim 300$ μm the available frequency differences ($\delta\nu = G\Delta_0$) cover the range of 5–150 GHz which is important for many applications.

(2) The WG mode frequency is subject to small modification by the coupling prism. Part of the evanescent field penetrates the prism changing the efficient refractive index and total length of the cavity. The increased losses due to reemission into the prism also vary the resonant frequency (as in any damped oscillator). The decay scale of WGM evanescent field outside the sphere is the same for both polarizations: $d^* = (\lambda/2\pi)(n^2-1)^{-1/2}$. However the confinements for TE and TM modes are not equal and so the values of the external fields are normalized to the corresponding internal fields. Therefore variation of the sphere–prism gap contributes to the change of $\delta\nu$. The magnitude of this effect can be evaluated as follows:

$$\frac{\mathrm{d}(\delta\nu)}{\nu\,\mathrm{d}d} = \frac{n^2-1}{\left[Q_{\mathrm{L}}^{\mathrm{TE}}(2d_0)\right]d^*},$$

where d_0 is the operating value of the gap, $Q_{\mathrm{L}}^{\mathrm{TE}}(2d_0)$ is the quality factor of the loaded WGM. With parameters of the sphere used in our experiments, the total 40 kHz drift of the beatnote between two lasers locked to adjacent orthogonal polarization modes must correspond to $\Delta d \approx 1$ nm, on the assumption that the observed instability was due to variation of the gap only.

(3) The drift of the current changes the laser frequency even with constant cavity mode frequencies. The tuning rate with the current is of the order of 10–30 kHz per μA. The current sources were well stabilized but current drift of about 1 μA over 15 min was possible.

Thus, all three described mechanisms might have contributed to the observed drift and further study is needed to separate them. It is obvious however from the above considerations that with proper stabilization of the gap, a microsphere with high-Q WG modes can be a basis of a competitive microwave-band optical-beatnote oscillator with temperature coefficient of frequency as low as 10^{-8} K.

7. Possible designs of a compact module

The line width of a DL coupled to a high-Q cavity does not depend on the distance between the laser and the cavity [5] (for reasonable distance of ≤ 1 m and high enough Q). This is valid also in our case since all relevant parameters – Q, coupling efficiency, and DL-WGMR distance – are similar to those of Ref. [5]. Thus, it is physically proved that a very compact DL-sphere module can be built with extremely high coherence. However the above described tabletop technical realization is far from being compact.

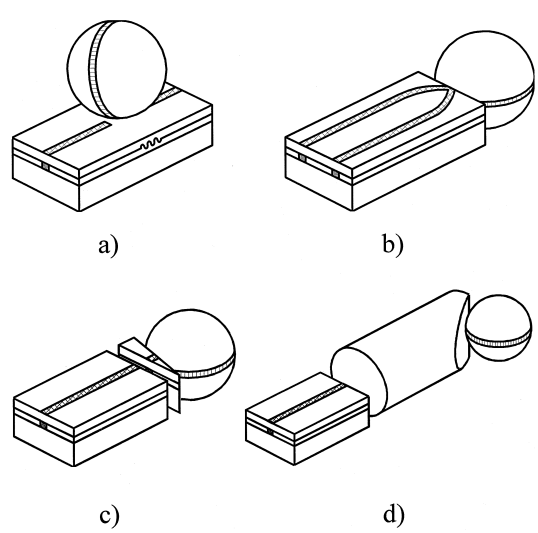

Fig. 9. The possible realizations of the compact high-coherent light source based on a diode laser and a whispering-gallery microresonator.

We see several possibilities to design a compact module. High refractive index and small cross section of the DL waveguide allows to couple laser mode and WG mode without intermediate bulky optical elements like prisms, objectives, etc. The angle of incidence to the semiconductor surface (from inside) should be equal to $\arcsin(n/n_{DL}) \approx 24°$. In the first version a short piece of grating is made along the passive part of the waveguide (similar to DBR laser) with one of its orders diffracted at 24° (Fig. 9a). The U-stripe scheme (Fig. 9b) seems to be simple; however, one of the end mirrors located on the same facet of the chip has to be made high reflective to prevent interference of the two output beams. A compact prism coupler can be based on the C^3-laser technology (Fig. 9c). Such a coupler having an independent electrical contact would also provide the control of the OFB phase. A half-pitch GRIN lens might be used instead of insertion lens and prism coupler (Fig. 9d). The contact zone can be prepared by polishing the rod-lens end at the appropriate angle [2].

8. Summary

The use of a 'whispering gallery' microresonator as an external high-Q cavity allows to diminish the DL line width by three orders down to 20 kHz, as demonstrated by the beatnote of two lasers optically locked to the WG modes having orthogonal polarizations. At the same time the line widths estimated both from the wings of the beatnote and the ratio of the tuning rates with and without feedback are of the order of 1 kHz which is close to results obtained with a bulky confocal interferometer. Since the effect of line width reduction does not depend on the distance between the sphere and DL, a kHz-line width laser can be built with very small dimensions. The stability of the beatnote frequency at the sampling time below 1 min was better than 4×10^{-6}, and at greater times the constant drift with the velocity of about 40 Hz/s limited stability. The possible contributions to the drift are analyzed. We also predict that temperature sensitivity of the frequency difference $\Delta\nu$ of the two orthogonally polarized modes depends on the sign and value of $\Delta\nu$ and can be made very small, allowing creation of high-stability microwave beatnote oscillator.

[2] Such a coupling was realized in our laboratory during preparation of the present manuscript and will be published elsewhere.

Acknowledgements

The authors gratefully acknowledge the financial support of the International Soros Foundation (grant MQR300) and of the Civil R&D Foundation (grant RP1 234) and thank I.B. Novikova and S.M. Il'ina for helpful discussions and technical assistance.

References

[1] M. Ohtsu, Highly Coherent Semiconductor Lasers, Artech House, Boston, 1992.
[2] E.M. Belenov, V.L. Velichansky, A.S. Zibrov, V.V. Nikitin, V.A. Sautenkov, A.V. Uskov, Sov. J. Quantum Electron. 13 (1983) 792.
[3] K.C. Harvey, C.J. Myatt, Opt. Lett. 16 (1991) 910.
[4] B. Dahmani, L. Hollberg, R. Drullinger, Opt. Lett. 12 (1987) 876.
[5] Ph. Laurent, A. Clairon, Ch. Breant, IEEE J. Quantum Electron. 25 (1989) 1131.
[6] A.G. Bulushev, E.M. Dianov, A.V. Kuznetsov, O.G. Okhotnikov, Sov. J. Quantum Electron. 13 (1989) 479.
[7] T.J. Paul, E.A. Swanson, Opt. Lett. 18 (1993) 1241.
[8] T. Day, F. Luecke, M. Brownell, Lasers and Optronics, June 1993, pp. 15–17.
[9] C.-H. Shin, M. Teshima, M. Ohtsu, T. Imai, J. Yoshida, K. Nishide, IEEE Photonics Technol. Lett. 2 (1990) 167.
[10] P.W. Smith, Proc. IEEE 60 (1972) 422.
[11] D.A. Ackerman, M.I. Dahbura, Y. Shani, C.H. Henry, R.C. Kistler, R.F. Kasarinov, C.Y. Kuo, Appl. Phys. Lett. 58 (1991) 449.
[12] V.B. Braginsky, M.L. Gorodetsky, V.S. Ilchenko, Phys. Lett. A 137 (1989) 393.
[13] V.L. Gorodetsky, A.A. Savchenkov, V.S. Ilchenko, Opt. Lett. 21 (1996) 453.
[14] H. Li, N.B. Abraham, Appl. Phys. Lett. 53 (1988) 2257.
[15] M. Ohtsu, H. Suzuki, K. Nemoto, Y. Teramachi, Jpn. J. Appl. Phys. 29 (1990) L1463.
[16] H.R. Simonsen, IEEE J. Quantum Electron. QE-29 (1993) 877.
[17] V.V. Vasil'ev, V.L. Velichanskii, M.L. Gorodetskii, V.S. Il'chenko, L. Hollberg, A.V. Yarovitskii, Quantum Electron. 26 (1996) 657.
[18] J.A. Stratton, Electromagnetic Theory, McGraw-Hill, New York, 1941.
[19] M.L. Gorodetsky, V.S. Ilchenko, Opt. Commun. 113 (1994) 133.
[20] S. Schiller, R.L. Byer, Opt. Lett. 16 (1991) 1138.
[21] V.S. Ilchenko, M.L. Gorodetsky, Laser Phys. 2 (1992) 1004.
[22] D.S. Weiss, V. Sandoghdar, J. Hare et al., Opt. Lett. 20 (1995) 1835.